
VIDEOADVISER: VIDEO KNOWLEDGE DISTILLATION FOR MULTIMODAL TRANSFER LEARNING

Yanan Wang^{1,2} Donghuo Zeng¹ Shinya Wada¹ Satoshi Kurihara²

¹KDDI Research ²Keio University

¹{wa-yanan, do-zeng, sh-wada}@kddi.com ²{wang-yanan, satoshi}@keio.jp

ABSTRACT

Multimodal transfer learning aims to transform pretrained representations of diverse modalities into a common domain space for effective multimodal fusion. However, conventional systems are typically built on the assumption that all modalities exist, and the lack of modalities always leads to poor inference performance. Furthermore, extracting pretrained embeddings for all modalities is computationally inefficient for inference. In this work, to achieve high efficiency-performance multimodal transfer learning, we propose *VideoAdviser*, a video knowledge distillation method to transfer multimodal knowledge of video-enhanced prompts from a multimodal fundamental model (teacher) to a specific modal fundamental model (student). With an intuition that the best learning performance comes with professional advisers and smart students, we use a CLIP-based teacher model to provide expressive multimodal knowledge supervision signals to a RoBERTa-based student model via optimizing a step-distillation objective loss—first step: the teacher distills multimodal knowledge of video-enhanced prompts from classification logits to a regression logit—second step: the multimodal knowledge is distilled from the regression logit of the teacher to the student. We evaluate our method in two challenging multimodal tasks: video-level sentiment analysis (MOSI and MOSEI datasets) and audio-visual retrieval (VEGAS dataset). The student (requiring only the text modality as input) achieves an MAE score improvement of up to **12.3%** for MOSI and MOSEI. Our method further enhances the state-of-the-art method by **3.4%** mAP score for VEGAS without additional computations for inference. These results suggest the strengths of our method for achieving high efficiency-performance multimodal transfer learning.

1 Introduction

Transfer learning is a promising methodology that focuses on transferring pretrained representation domains to nearby target domains Zhuang et al. [2021]. For instance, finetuning a pretrained language model on a small annotated dataset enables high-performance text sentiment analysis Hazarika et al. [2020]. Recent fundamental models on diverse modalities such as language models (e.g., RoBERTa Liu et al. [2019], GPT-3 Brown et al. [2020]), visual models (e.g., ViT Dosovitskiy et al. [2021]), and multimodal models (e.g., CLIP Radford et al. [2021], MEET Nie et al. [2022]) have millions of parameters and can provide robust modal representations. With such advancement, multimodal transfer learning aims to transform pretrained representations of diverse modalities into a common domain space for effective multimodal fusion Zhen et al. [2022], Albanie et al. [2018]. It has been broadly applied to multimodal tasks such as video-level sentiment analysis Yu et al. [2021], Han et al. [2021a], Hu et al. [2022], and audio/text-video retrieval tasks Zeng et al. [2020], Zhen et al. [2019], Han et al. [2021b], Zeng et al. [2022].

Existing works on multimodal transfer learning unify adversarial learning to regularize the embedding distributions between different modalities, leading to effective multimodal fusion He et al. [2017], Wang et al. [2017], Zhang et al. [2017], Zhen et al. [2019], Wang et al. [2022]. However, conventional systems are typically built on the assumption that all modalities exist, and the lack of modalities always leads to poor inference performance. For instance, vision-language models typically fail to achieve expected performance when given only text data as input. Furthermore, extracting pretrained embeddings for all modalities is computationally inefficient for inference. Therefore, improving robust

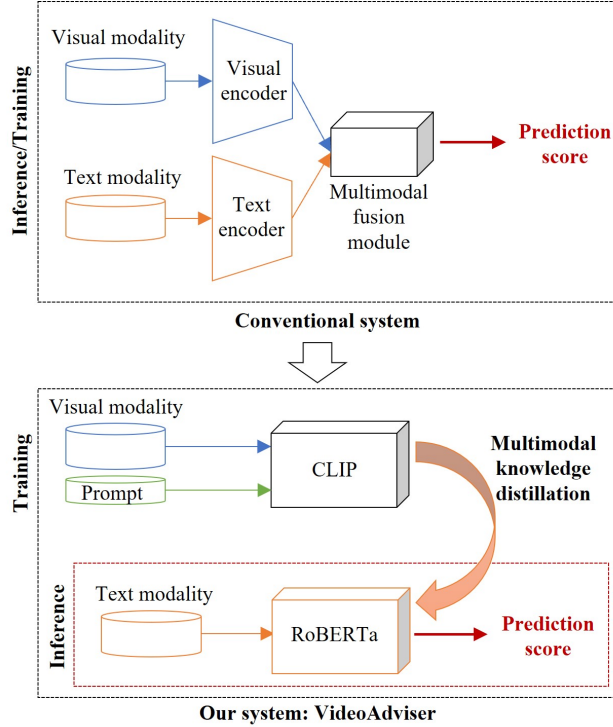


Figure 1: A conceptual diagram illustrates the difference between the conventional system and our system: our system focuses on transferring multimodal knowledge from a multimodal fundamental model (e.g., CLIP) to a language fundamental model (e.g., RoBERTa-Large), and requires text only to achieve high efficiency-performance inference. On the other hand, the conventional system focuses on multimodal fusion and requires complex modules (diverse modal encoders and a multimodal fusion module) for inference.

multimodal transfer learning to achieve high efficiency-performance inference is crucial for practical applications, which motivates this work.

Knowledge distillation (KD) is first proposed for achieving an efficient student model by transforming embedded knowledge in the predicted logits of the teacher model to a smaller student model Hinton et al. [2015]. Recent works have expanded it to multimodal transfer learning by distilling mutual information from one modality to another Gupta et al. [2016], Thoker and Gall [2019], Jiao et al. [2020], Hou et al. [2020], Pan et al. [2020]. However, these works always need to sacrifice the performance of the teacher model, requiring the teacher model and the student model distributed in neighboring domains (e.g., vision \rightarrow vision, text \rightarrow text).

In this paper, with an intuition that the best learning performance comes with professional advisers and smart students, to achieve high efficiency-performance multimodal knowledge distillation, we propose *VideoAdviser* shown in Figure 1, a video knowledge distillation method to transfer multimodal knowledge from a strong multimodal fundamental model (teacher) to a powerful specific modal fundamental model (student) via optimizing a step-distillation objective loss. As CLIP is a multimodal fundamental model pretrained with cross-modal contrastive learning on tremendous image-text pairs Radford et al. [2021], we employ it as the teacher model to obtain multimodal knowledge of video-enhanced prompts by incorporating the video and text prompt representations. The teacher model utilizes CLIP’s visual and text encoders to obtain video and text prompt embeddings without freezing the pretrained weights to preserve multimodal representation space learned by CLIP. By adapting transformer-based modules on these embeddings and extracted frame-level facial expression features, the teacher model acquires expressive multimodal knowledge of video-enhanced prompts by performing video and text prompt representations learning. To sufficiently absorb distilled multimodal knowledge from the teacher model, we employ a large-scale language model RoBERTa Liu et al. [2019] as the student model. Since RoBERTa is a transformer-based architecture composed of huge parameters, we finetune its full parameters to leverage RoBERTa’s powerful architecture to achieve high-performance student models for inference. In addition, we propose a step-distillation objective loss to distill coarse-fine grained multimodal knowledge to further improve the multimodal knowledge distillation. Motivated by multiscale representation learning enabling the fusion of enriched coarse-fine grained representations Li et al. [2022], Jiao et al. [2023], we consider that multitask with different target

granularities allows the model to acquire representative knowledge at diverse granularities. For instance, classification encourages the model to separate the data point into multiple categorical classes representing an interval of consecutive real values to acquire knowledge at a coarse granularity. In contrast, regression enables the model to distinguish the data point into continuous real values instead of using classes to learn knowledge at a fine granularity. To this end, in the first step, the teacher model distills multimodal knowledge of video-enhanced prompts from classification logits to a regression logit to unify knowledge at both coarse and fine granularity; In the second step, the unified multimodal knowledge is further distilled from the teacher model to the student model.

We evaluate *VideoAdviser* in two challenging multimodal tasks: video-level sentiment analysis (MOSI and MOSEI datasets) and audio-visual retrieval (VEGAS dataset). The RoBERTa-based student model requiring only text data as input outperforms the state-of-the-art multimodal model’s MAE score by **12.3%** for MOSI and **2.4%** for MOSEI. Our method also enhances the state-of-the-art audio-visual cross-modal model by **3.4%** mAP score for VEGAS without additional computations for inference. Ablation studies further demonstrate that our method is able to improve the state-of-the-art method’s MAE score by over **3.0%** with almost half the parameters. These results suggest the strengths of our method for achieving high efficiency-performance multimodal transfer learning.

2 Related work

2.1 Multimodal fundamental model

CLIP Radford et al. [2021] is a multimodal fundamental model that learns transferable visual models from natural language supervision on a dataset of 400 million (image, text) pairs. It jointly trains an image encoder and a text encoder using contrasting learning objectives to obtain a joint multimodal representation space. Inspired by its remarkable zero-shot generation ability for downstream image tasks, the work Ni et al. [2022] proposes XCLIP to expand pretrained CLIP on general video recognition by finetuning it on video data using a video-specific prompting module that enhances the video representation to the text representation. The work Gu et al. [2021] utilizes a pretrained CLIP for open-vocabulary object detection by distilling visual knowledge from cropped image regions. In this work, we adapt a pretrained CLIP on distilling multimodal knowledge of video-enhanced prompts from the teacher model to the student model via a step-distillation objective loss.

2.2 Knowledge distillation based transfer Learning

In addition to achieving a lightweight student model by minimizing the KL divergence between the probabilistic outputs of a teacher and student model Hinton et al. [2015], recent works on knowledge distillation focus on transferring representational knowledge from a teacher model to a student model Tian et al. [2020], Gu et al. [2021], Wang and Yoon [2022]. For instance, these works Wang et al. [2020a,b] distill linguistic knowledge from a text encoder to a visual encoder by learning the mapping between modal representations. The work Croitoru et al. [2021] utilizes multiple text encoders to perform cross-modal knowledge distillation for stronger text-video retrieval. The work Dai et al. [2022] distills expressive text representations from a generation model to the text encoder of CLIP by minimizing text-text feature distance. However, these works mostly focus on knowledge distillation in the common modal domain or show limited performance in the cross-modal domain. In contrast, to achieve expressive knowledge distillation for multimodal transfer learning tasks, we propose a RoBERTa-based student model to improve multimodal knowledge distillation by leveraging its powerful transformer architecture.

2.3 Video-level sentiment analysis task

Recent works Hazarika et al. [2020], Han et al. [2021a], Yu et al. [2021] on video-level sentiment analysis tasks focus on improving modality fusion. The work Wang et al. [2017] proposes VAE-Based adversarial learning method to map multimodal representations to a joint domain space for improving the modality fusion process. The work Hu et al. [2022] achieves SOTA performance on MOSI Zadeh et al. [2016] and MOSEI Bagher Zadeh et al. [2018] dataset by introducing a pretrained modality fusion module that fuses multimodal representation from multi-level textual information by injecting acoustic and visual signals into a text encoder. However, all these works require preprocessed multimodal embeddings as the input which is inefficient for inference. In contrast, we employ a knowledge distillation approach that requires only one specific modality leading to efficient inference.

2.4 Audio-visual retrieval task

Recent works on audio-visual retrieval tasks exploit supervised representation learning methods to generate new features across modalities in a common space Han et al. [2021b], Rasiwasia et al. [2014], Zeng et al. [2018], Zheng et al. [2020],

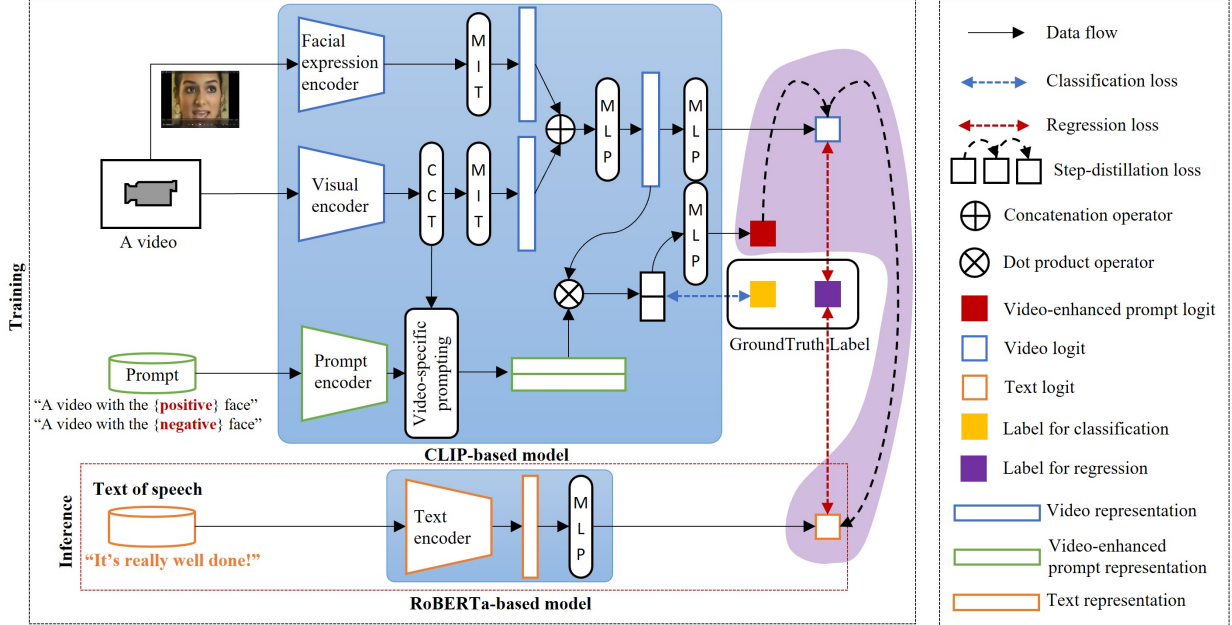


Figure 2: Architecture of *VideoAdviser* using a CLIP-based model (the teacher) to distill multimodal knowledge of video-enhanced prompts to a RoBERTa-based model (the student): the teacher model utilizes pretrained CLIP’s text and visual encoders, and a facial expression encoder to obtain the sentiment class text embedding, the frame-level embedding, and the facial expression embedding. Then, the teacher model employs CCT, MIT, MLP, and a video-specific prompting module, and minimizes a binary sentiment classification loss and a sentiment regression loss. Meanwhile, the student model is finetuned on speech text by minimizing a sentiment regression loss and a step-distillation loss (the region in purple). During inference, the speech text is used to enable sentiment intensity prediction. Here, CCT, MIT, and MLP stand for the cross-frame communication transformer, multi-frame integration transformer, and multi-layer perceptron, respectively.

Zhen et al. [2019], Zeng et al. [2020, 2022, 2023], such that the audio-visual features can be measured directly. Inspired by the C-CCA Rasiwasia et al. [2014] that aims at finding linear transformations for each modality, C-DCCA Zeng et al. [2018] tries to learn non-linear features in the common space by using deep learning methods. Deep learning methods by using rank loss to optimize the predicted distances, such as TNN-C-CCA Zeng et al. [2020], and CCTL Zeng et al. [2022] models, which apply triplet losses as the objective functions to achieve better results than other CCA-variant methods. The EICS model Zeng et al. [2023] learns two different common spaces to capture modality-common and modality-specific features, which achieves the SOTA results so far. In this paper, we enable our method to enhance the extracted audio and visual representations of the SOTA model by distilling multimodal knowledge from a CLIP-based teacher model.

3 Problem setting

This work focuses on video-level sentiment analysis and audio-visual retrieval tasks, respectively. For the video-level sentiment analysis task, each data point consists of a video M , the cropped sequential face images I , the divided speech text T_{speech} , and the class text T_{class} , our goal is to predict the sentiment intensity $Z_{pred} \in [-3, 3]$ by giving only speech text T_{speech} for inference. For the audio-visual retrieval task, assume that $\Gamma = \{\gamma_i\}_{i=1}^N$ is a video collection, $\gamma_i = \{a_i, v_i\}$, where N indicates the data size, $a_i \in \mathbb{R}^{D1}$ and $v_i \in \mathbb{R}^{D2}$ are audio and visual features from different feature spaces. Our target aims at feeding them into a common space by mapping functions $f(x)$ and $g(x)$ to generate new features $f(a_i)$ and $g(v_i)$. As a result, each query a_i for example will obtain a rank list from another modality based on $query-v_j (i \neq j)$ similarity.

4 Methodology

In this section, we explain our method *VideoAdviser* in detail. As shown in Fig. 2, our method consists of a CLIP-based model as the teacher (§ 4.1) and a RoBERTa-based model as the student (§ 4.2). The teacher and student models are

jointly trained to achieve knowledge distillation across modalities. The student model enables sentiment intensity prediction by giving only a speech text for inference (§ 4.3). We use $\mathcal{F}(\cdot)$, $\mathcal{V}(\cdot)$, $\mathcal{P}(\cdot)$ and $\mathcal{T}(\cdot)$ to denote the facial expression encoder, visual encoder, prompt encoder, and text encoder.

4.1 The CLIP-based teacher model

Facial expression embedding To enhance the visual representations of the teacher model for sentiment intensity prediction, we first use OpenFace Baltrušaitis et al. [2016] to crop face images $\{I_i\}_{i=1}^T \in \mathbb{R}^{P^2 \times 3}$ with each of size $P \times P$ pixels from T sampled video frames, then, we extract frame-level facial expression embedding $\mathbf{v}^{(f)} \in \mathbb{R}^{T \times D}$ with a facial expression encoder $\mathcal{F}(\cdot)$ Albanie and Vedaldi [2016] that is pretrained on the VGG-Face dataset Parkhi et al. [2015]. Here, $\mathbf{v}^{(f)}$ is an 8-dimensional sequential vector of length 64 [$T = 64$, $D = 8$]. More details of the pretrained model on Albanie’s website ¹.

$$\mathbf{v}^{(f)} = \mathcal{F}(\{I_i\}_{i=1}^T) \quad (1)$$

Visual embedding To fully transfer the powerful generality of pretrained CLIP Radford et al. [2021] from image to video, we freeze the parameters of pretrained CLIP visual encoder $\mathcal{V}(\cdot)$ to obtain frame-level visual embedding $\mathbf{v}^{(v)} \in \mathbb{R}^{T \times D}$, where T denotes the number of sampled video frames and D is the dimension of visual embedding. Following Ni et al. [2022], given a video clip $M \in \mathbb{R}^{T \times H \times W \times 3}$ of T sampled video frames with $H \times W$ pixels, we use ViT-L/14 Dosovitskiy et al. [2021] to first divide t -th frame into N patches $\{x_{t,i}\}_{i=1}^N \in \mathbb{R}^{P^2 \times 3}$, where $t \in T$ and $N = HW/P^2$. Then, the patches $\{x_{t,i}\}_{i=1}^N$ is mapped to $\mathbf{v}^{(v)} = \{v_t^{(v)}\}_{t=1}^T$ with a linear transformation $f_m : \mathbb{R}^{P^2 \times 3} \rightarrow \mathbb{R}^{3P^2 \times D}$.

$$\mathbf{v}^{(v)} = \mathcal{V}(f_m(\{\mathbf{x}_t\}_{t=1}^T)) \quad (2)$$

Text prompt embedding We employ the text encoder $\mathcal{P}(\cdot)$ of pretrained CLIP to obtain text prompt embedding $\mathbf{v}^{(p)} \in \mathbb{R}^{C \times D}$ of C sentiment classes by giving the sentiment class label $T_{class} \in \{\text{negative, positive}\}$, where “positive” class includes 0. The text prompt such as “A video with the $\{T_{class}\}$ face” is generated with a text prompt generator f_g and encoded as

$$\mathbf{v}^{(p)} = \mathcal{P}(f_g(T_{class})) \quad (3)$$

We employ the cross-frame communication transformer (CCT), multi-frame integration transformer (MIT), and video-specific prompting modules to obtain expressive multimodal sentiment knowledge. The CCT is a multi-layer transformer with cross-frame attention introduced in Ni et al. [2022] to enable cross-frame information exchange. It is used to obtain cross-frame visual representations by giving a modified visual embedding $\bar{\mathbf{v}}^{(v)} = \{\bar{v}_t^{(v)}\}_{t=1}^T$, where $\bar{v}_t^{(v)} = [x_{class}, v_t^{(v)}] + e_{pos}$. x_{class} is a learnable frame representation and e_{pos} is a position embedding of patches in a frame. The MIT is a normal transformer layer constructed by standard multi-head self-attention and feed-forward networks. Given frame-level embeddings $\mathbf{v}^{(f)}$ and $\bar{\mathbf{v}}^{(v)}$, we finally obtain the video representation V as follows:

$$V^{(f)} = \text{AvgPool}(\text{MIT}(\mathbf{v}^{(f)})) \quad (4)$$

$$V^{(v)} = \text{AvgPool}(\text{MIT}(\text{CCT}(\bar{\mathbf{v}}^{(v)}))) \quad (5)$$

$$V = f_v([V^{(f)} || V^{(v)}]) \quad (6)$$

where $f_v : \mathbb{R}^{2D} \rightarrow \mathbb{R}^D$ is a two-layer MLP. AvgPool denotes an average pooling layer. “||” denotes a concatenation operator used to process facial expression-conditioned video representation. We then transform the **video representation** V to the **video logit** (see Fig. 2) with a two-layer MLP.

Inspired by Ni et al. [2022], the teacher model employs a video-specific prompting module to enhance the prompt embedding with cross-frame visual representations. The video-specific prompting module applies a normal multi-head attention Vaswani et al. [2017] to obtain the **video-enhanced prompt representation** $\bar{\mathbf{v}}^{(p)} \in \mathbb{R}^{C \times D}$ (see Fig. 2) as

$$\bar{\mathbf{v}}^{(p)} = \mathbf{v}^{(p)} + \text{Multi_Hand_Attention}(\text{CCT}(\bar{\mathbf{v}}^{(v)})) \quad (7)$$

Then, we compute dot product between video representation V and video-specific prompt representation $\bar{\mathbf{v}}^{(p)} = \{\bar{v}_i^{(p)}\}_{i=1}^C$ to output the similarity score $\mathbf{p} = \{p_i\}_{i=1}^C$ with a softmax layer as

$$p_i = \text{softmax}(\bar{v}_i^{(p)} \cdot V) = \frac{\exp(\bar{v}_i^{(p)} \cdot V)}{\sum_{i \in C} \exp(\bar{v}_i^{(p)} \cdot V)} \quad (8)$$

¹<https://www.robots.ox.ac.uk/~albanie/mcn-models.html>

where C indicates the number of sentiment classes. We further transform \mathbf{p} into the **video-enhanced prompt logit** (see Fig. 2) with a two-layer MLP.

4.2 The RoBERTa-based student model

To leverage the powerful transformer-based architecture of fundamental language models, we structure a RoBERTa-based student model Liu et al. [2019] that consists of a text encoder $\mathcal{T}(\cdot)$ and a two-layer MLP. Given the speech text T_{speech} , the student model obtains text representation $V^{(t)}$ with $\mathcal{T}(\cdot)$, and output sentiment intensity \mathcal{Z}_{pred} with the MLP into the **text logit** (see Fig. 2) as

$$\mathcal{Z}_{pred} = \text{logit}(V^{(t)}), V^{(t)} = \mathcal{T}(T_{speech}) \quad (9)$$

Where $V^{(t)} \in \mathbb{R}^D$, and $\text{logit}(\cdot) : \mathbb{R}^D \rightarrow \mathbb{R}^1$ indicates the two-layer MLP.

4.3 Training objectives

We simultaneously optimize the teacher and student models by applying mean squared error (MSE) loss to obtain video and text sentiment knowledge. Both teacher and student models minimize the L_2 distance as follows:

$$\mathcal{L}_v^{(r)} = \text{MSE}(\text{logit}(V), l^{(r)}) = \frac{1}{B} \sum_{i=1}^B \|\text{logit}(V) - l^{(r)}\|^2 \quad (10)$$

$$\mathcal{L}_t^{(r)} = \text{MSE}(\mathcal{Z}_{pred}, l^{(r)}) = \frac{1}{B} \sum_{i=1}^B \|\mathcal{Z}_{pred} - l^{(r)}\|^2 \quad (11)$$

where B indicates batch size, $\mathcal{L}_v^{(r)}$ indicates MSE between the teacher model’s video logit and sentiment label $l^{(r)}$, and $\mathcal{L}_t^{(r)}$ indicates MSE between the student model’s text logit (\mathcal{Z}_{pred}) and $l^{(r)}$. Here, $\text{logit}(V)$ is a two-layer MLP for transforming video representation V into the video logit.

To learn the video-enhanced prompt representation to fuse multimodal knowledge of video and class text, we use the binary sentiment classification label $l^{(c)}$ (see Fig. 3) synthesized from the sentiment label to optimize the teacher model with a cross-entropy loss $\mathcal{L}_v^{(c)}$ as

$$\mathcal{L}_v^{(c)} = - \sum_{i=1}^C l_i^{(c)} \log(p_i), \quad (12)$$

We optimize a step-distillation objective loss to achieve multimodal knowledge distillation from the teacher model to the student model. The step-distillation objective loss consists of a **prompt-video distance minimization** $\mathcal{L}_{p \rightarrow v}$ and a **video-text distance minimization** $\mathcal{L}_{v \rightarrow t}$, where $\mathcal{L}_{p \rightarrow v}$ is optimized to align coarse-grained classification knowledge in the video-enhanced prompt logit and fine-grained regression knowledge in the video logit, $\mathcal{L}_{v \rightarrow t}$ is optimized to align knowledge in the video logit of the teacher model and the text logit of the student model. We apply MSE loss to perform the step-distillation as follows:

$$\mathcal{L}_{p \rightarrow v} = \text{MSE}(\text{logit}(\mathbf{p}), \text{logit}(V)) \quad (13)$$

$$\mathcal{L}_{v \rightarrow t} = \text{MSE}(\text{logit}(V), \mathcal{Z}_{pred}) \quad (14)$$

where $\text{logit}(\mathbf{p})$ indicates the coarse-grained classification knowledge in Eq. 12.

We finally have a joint loss \mathcal{L} for training the teacher and student models end-to-end as

$$\mathcal{L} = \alpha \mathcal{L}_v^{(r)} + \beta \mathcal{L}_t^{(r)} + \gamma \mathcal{L}_v^{(c)} + \delta \mathcal{L}_{p \rightarrow v} + \psi \mathcal{L}_{v \rightarrow t} \quad (15)$$

where $\alpha, \beta, \gamma, \delta$, and ψ indicate the importance of each loss value. They are empirically set as 1 : 10 : 1 : 10 : 1 to keep all loss values on the same scale.

5 Experiment

In this section, we conducted empirical experiments on video-level sentiment analysis and audio-visual retrieval tasks to demonstrate the high efficiency-performance of our method.

5.1 Dataset

MOSI Zadeh et al. [2016] and MOSEI Bagher Zadeh et al. [2018] are multimodal datasets collected from online video for evaluating video-level sentiment analysis tasks. We show the dataset size in Tab. 1. MOSEI drops the data lacking modalities to fairly evaluate recent modality fusion-based methods Wang et al. [2022]. We compared the video segment IDs of each data point for each modality and saved only the data points associated with a common segment ID. The modified MOSEI dataset was found to be more challenging than the original dataset as it lowered the strong baseline MSE score by 4.9% (see Tab. 2). Both datasets are annotated with a Likert scale in the range of $[-3, 3]$, *i.e.*, (-3: highly negative, -2: negative, -1: weakly negative, 0: neutral, +1: weakly positive, +2: positive, +3: highly positive). We further synthesize binary classification label, *i.e.*, $[-3, 0)$: negative, $[0, 3]$: non-negative) used for optimizing the teacher model (§4.1). The label distribution is illustrated in Fig. 3. MOSEI is imbalanced and over 65% of data is distributed in $[-1, 1]$.

VEGAS dataset Zhou et al. [2018] is applied for the audio-visual retrieval task, which contains 28,103 videos in total as shown in Tab. 1. Each video can be embedded as an audio feature vector and a visual feature vector, and the audio-visual pair shares the same single label. The label represents an audio event (*e.g.*, baby crying) of the human voice or natural sound. The number of label classes is 10, and the length of each audio-visual pair ranges from 2 to 10 seconds.

Table 1: Dataset size. MOSEI uses the same dataset as Wang et al. [2022].

| Dataset | Train | Validation | Test | Total |
|----------------------------------|--------|------------|-------|--------|
| MOSI Zadeh et al. [2016] | 1,284 | 229 | 686 | 2,199 |
| MOSEI Bagher Zadeh et al. [2018] | 9,473 | 1,206 | 2,710 | 13,389 |
| VEGAS Zhou et al. [2018] | 22,482 | - | 5,621 | 28,103 |

5.2 Evaluation metric

We use the mean absolute error (MAE), accuracy (A^7), accuracy (A^2), and weight- $F1$ score for evaluating MOSI and MOSEI. A^7 denotes a 7-class and A^2 denotes a binary accuracy metric. Since MOSI and MOSEI are regression problems, we consider MAE to be the most reasonable metric for fair evaluations. In addition to the binary accuracy reported by most of the previous works, we evaluate the 7-class accuracy as did the SOTA method Hu et al. [2022] to eliminate the effect of the data imbalance. For the audio-visual retrieval task, we apply the mean average precision (mAP) as previous works Zeng et al. [2023, 2022] to evaluate our model.

5.3 Training setting

We train the teacher and the student models simultaneously and use only the student model for inference. The text modality is used for evaluating MOSI and MOSEI. On the other hand, as shown in Fig. 4, we utilize the teacher model to distill multimodal knowledge for both visual and audio encoders of the state-of-the-art model EICS Zeng et al. [2023] for audio-visual retrieval tasks. Both visual and audio encoders are used as student models to evaluate VEGAS. We show the hyperparameters of *VideoAdviser* (§4) for both tasks in detail in Tab. 3.

5.4 Performance

5.4.1 Evaluation of video-level sentiment analysis

We compared *VideoAdviser* with strong baseline methods on the test set of MOSI and MOSEI in Tab. 2. Compared with the state-of-the-art method UniMSE Hu et al. [2022] that utilizes the powerful architecture of a large-scale pretraining model T5 Raffel et al. [2020] to improve the multimodal fusion by embedding multimodal signals into an auxiliary layer of T5, *VideoAdviser* is a multimodal knowledge distillation-based method that distills multimodal knowledge from a multimodal fundamental model CLIP Ni et al. [2022] to a language model RoBERTa Liu et al. [2019]. UniMSE was trained by integrating the training datasets of MOSI, MOSEI, MELD Poria et al. [2019], IEMOCAP Busso et al. [2008] and multimodal signals are required for inference. In contrast, our method was trained using the target dataset and requires only text data for inference. *VideoAdviser* significantly improves UniMSE’s MAE score by **12.3%** for MOSI, and outperforms a strong baseline method VAE-AMDT’s MAE score by **2.4%** for MOSEI. As we use the teacher model to offer auxiliary multimodal supervision signals to the student model, by leveraging the strengths of the learned multimodal space of the teacher model and the large-scale parameters of the student model, we think our method

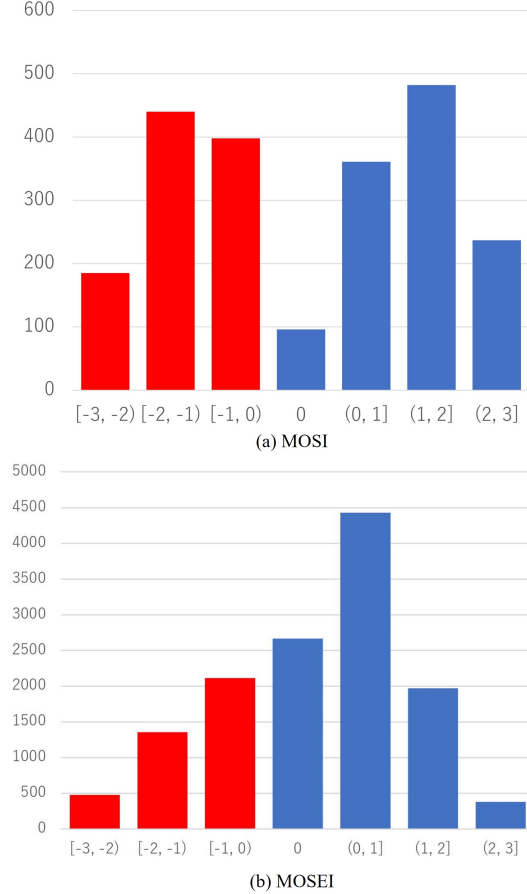


Figure 3: Label distribution of (a) MOSI and (b) MOSEI. The synthesized binary classification label is illustrated in different colors (the “negative” class in red color and the “non-negative” class in blue color).

Table 2: Comparison results for MOSI and MOSEI. Our model reduces the state-of-the-art UniMSE’s MAE score by **12.3%** for MOSI, and VAE-AMDT’s MAE by **2.4%** for MOSEI. Here, (\downarrow) indicates the lower the MAE, the better the performance, and (\uparrow) indicates the vice-versa. (*) indicates the results produced on the modified MOSEI dataset.

| Model | MOSI | | | | | MOSEI | | | | |
|-------------------------------|------------------|------------------|------------------|---------------|-----------------|------------------|------------------|------------------|---------------|-----------------|
| | MAE \downarrow | A^7 \uparrow | A^2 \uparrow | F1 \uparrow | Corr \uparrow | MAE \downarrow | A^7 \uparrow | A^2 \uparrow | F1 \uparrow | Corr \uparrow |
| MISA Hazarika et al. [2020] | 0.804 | - | 80.8 | 80.8 | 0.764 | 0.568 | - | 82.6 | 82.7 | 0.717 |
| VAE-AMDT Wang et al. [2022] | 0.716 | - | 84.3 | 84.2 | - | 0.526* | - | 82.8* | 87.5* | - |
| MAG-BERT Rahman et al. [2020] | 0.712 | - | 84.2 | 84.1 | 0.796 | 0.539 | - | 84.7 | 84.5 | - |
| Self-MM Yu et al. [2021] | 0.713 | - | 84.0 | 84.4 | 0.798 | 0.530/0.579* | - | 82.8/84.6* | 82.5/84.6* | 0.765/- |
| MMM Han et al. [2021a] | 0.700 | 46.7 | 84.1 | 84.0 | 0.800 | 0.526 | 54.2 | 82.2 | 82.7 | 0.772 |
| UniMSE Hu et al. [2022] | 0.691 | 48.7 | 85.9 | 85.3 | 0.809 | 0.523 | 54.4 | 85.9 | 85.8 | 0.773 |
| VideoAdviser (ours) | 0.568 | 51.3 | 87.7 | 87.9 | 0.872 | 0.502* | 54.5* | 84.5* | 85.0* | 0.810* |
| Human | 0.710 | - | 85.7 | 87.5 | 0.820 | - | - | - | - | - |

is effective for achieving high-performance multimodal knowledge distillation via minimizing the step-distillation objective loss (§4.3).

5.4.2 Evaluation of audio-visual retrieval

We further evaluated our *VideoAdviser* on the VEGAS dataset in Tab. 4. Compared to the state-of-the-art method EICS Zeng et al. [2023] that builds two different common spaces to learn the modality-common and modality-specific

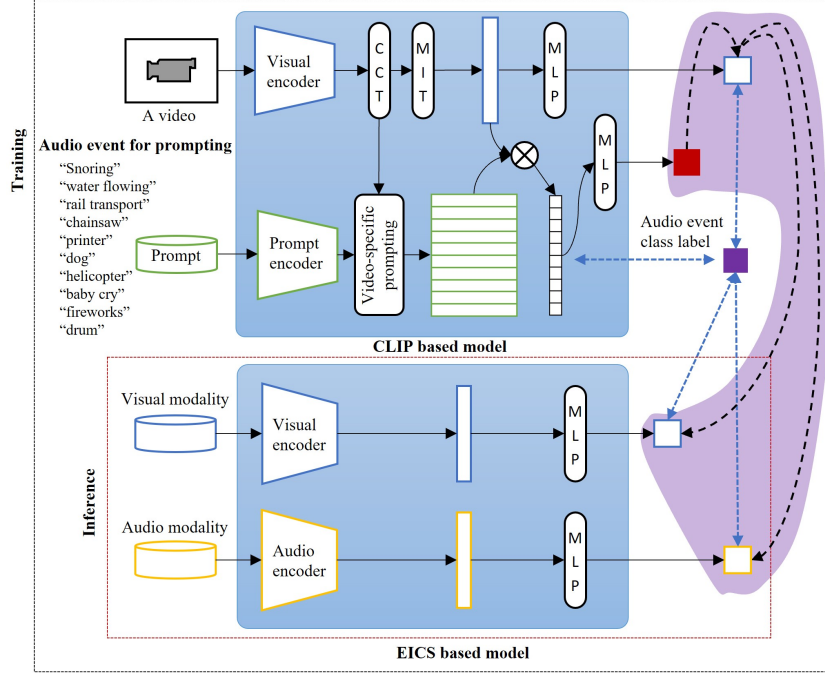


Figure 4: Architecture of *VideoAdviser* for audio-visual retrieval task using a CLIP-based model (the teacher) to distill multimodal knowledge of video-enhanced prompts to an EICS-based audio-visual model (the student). The teacher model is finetuned for the audio event classification to distill multimodal knowledge to the student model via the step-distillation loss (the region in purple). We adopt 3-layer MLP with 128-dimensional hidden layers.

features, which achieves an average mAP of 0.788. Our method utilizes the distilled multimodal knowledge to enhance the performance of EICS. As a result, it achieves an average mAP of 0.822 and improves EICS Zeng et al. [2023] by 3.4%, suggesting the generality of our method on audio-visual retrieval tasks.

5.5 Efficiency

By comparing the number of parameters with state-of-the-art models in Fig. 5, our proposed *VideoAdviser* requires only a language model as the student that is able to achieve a high efficiency-performance model for inference. The Student (BERT Devlin et al. [2019]) achieved a compatible MAE score with fewer parameters than previous BERT-based models. Moreover, these models always process visual and audio signals for multimodal fusion, which might require more parameters and increase the computation cost. Compared with the state-of-the-art model UniMSE that uses a pretrained transformer-based language model T5 Raffel et al. [2020] to perform multimodal fusion, our model, the student (ROBERTa-Base Liu et al. [2019]) with nearly half of the parameters reduces MAE score of over 3.0 point, suggesting the high efficiency-performance of our method. *VideoAdviser* was further improved over 9.0 point by adopting a RoBERTa-Large model as the student model.

5.6 Analysis

5.6.1 Effectiveness of components of the teacher model

We studied the effects of two core components of the teacher model (Facial expression encoder and video-specific prompting module) in Tab. 6. The results show that these two components help improve the multimodal knowledge distillation and boost the final performance of the student model. We believe that the facial expression encoder provided extra visual knowledge, and the video-specific prompting module further associated visual knowledge with text prompt representations encoded by the prompt encoder.

5.6.2 Effectiveness of the student model

We studied the effects of *VideoAdviser* on different student models in Tab. 7. We select two language models (BERT and RoBERTa) that have frequently been used in recent works Hazarika et al. [2020], Wang et al. [2022], Rahman

Table 3: The hyperparameters for training *VideoAdviser*. Here, “B” denotes the batch size, “Audio logit” denotes the output of the audio encoder for VEGAS (see Fig. 4).

| | Hyperparameter | MOSI, MOSEI | VEGAS |
|--------------|-------------------------------|-----------------------------|------------|
| Video | visual encoder | ViT-L/14 | |
| | Num. of frames | 8 | |
| | Frame size | 224×224 | |
| | visual embedding size (input) | (B, 64, 8) | (B, 1, 10) |
| | Visual hidden layer size | (B, 128) | |
| Prompt | Prompt encoder | ClipTextModel | |
| | Prompt embedding size (input) | (B,77,512) | |
| | Prompt hidden layer size | 128 | |
| Text | Text encoder | RoBERTa-large | - |
| | Text embedding size (input) | (B,100,1024) | - |
| | Text hidden layer size | 128 | - |
| Audio | Audio encoder | - | EICS model |
| | Audio feature size (input) | - | 10 |
| | audio hidden layer size | - | 128 |
| Output logit | Video-enhanced prompt logit | (B, 1) | (B, 10) |
| | Video logit | (B, 1) | (B, 10) |
| | Text logit | (B, 1) | - |
| | Audio logit | - | (B, 10) |
| Optimizer | Method | AdamW Kingma and Ba [2015] | |
| | Learning rate | 8e-6 | |
| | Warmup steps | 15 | |
| | Scheduler | cosine_schedule_with_warmup | |
| Training | GPU | GTX 1080 Ti | |
| | Batch size | 4 | |
| | Training epochs | 100 | |

et al. [2020], Yu et al. [2021], Han et al. [2021a]. By comparing the performance of language models with and without adopting a teacher model, the results demonstrate that our method improves a general language model’s MAE score by over **6.0** point on average, suggesting the efficacy and generality of our method with different student models. We consider that the teacher model offers auxiliary multimodal supervision to the student model during training, the language model-based students are able to learn multimodal knowledge from the teacher with their large-scale parameters.

We further trained a student model by freezing pretrained parameters, which dramatically dropped the MAE score from 0.568 to 1.478. This result makes us believe that in order to achieve expressive multimodal knowledge distillation across modalities, it is essential to finetune full parameters to leverage the strengths of large-scale pretrained models with powerful representational learning capabilities.

5.6.3 Modality effectiveness

To confirm the robustness of *VideoAdviser* in multimodal knowledge distillation not only for text modality but also for diverse modalities such as visual and audio modalities, we respectively studied the effects on visual and audio modalities for audio-visual retrieval tasks. As the results indicated in Tab. 8, the proposed step-distillation works for both modalities by boosting the baseline EICS model by over 1% mAP score. By associating both sides, we finally improved the baseline by 3.4%.

Table 4: The mAP comparison results with state-of-the-art models for VEGAS. Here, “V” and “A” indicate “Video” and “Audio”, respectively.

| Model | VEGAS | | |
|-------------------------------|--------------|--------------|--------------|
| | A→V | V→A | Average |
| Random | 0.110 | 0.109 | 0.109 |
| BiC-Net Han et al. [2021b] | 0.680 | 0.653 | 0.667 |
| C-CCA Rasiwasia et al. [2014] | 0.711 | 0.704 | 0.708 |
| C-DCCA Yu et al. [2019] | 0.722 | 0.716 | 0.719 |
| DCIL Zheng et al. [2020] | 0.726 | 0.722 | 0.724 |
| DSCMR Zhen et al. [2019] | 0.732 | 0.721 | 0.727 |
| TNN-C-CCA Zeng et al. [2020] | 0.751 | 0.738 | 0.745 |
| CCTL Zeng et al. [2022] | 0.766 | 0.765 | 0.766 |
| EICS Zeng et al. [2023] | 0.797 | 0.779 | 0.788 |
| VideoAdviser (ours) | 0.825 | 0.819 | 0.822 |

Table 5: Efficiency comparison. *VideoAdviser* is able to train a high efficiency-performance student model compared to state-of-the-art methods for inference. The student (RoBERTa-Base) outperforms the SOTA by over **3.0** point with nearly half the parameters.

| Model | Parameters | MOSI |
|---------------------------------|-------------|--------------|
| | | MAE |
| BERT-based model | | |
| - MISA Hazarika et al. [2020] | >110M | 0.804 |
| - MAG-BERT Rahman et al. [2020] | >110M | 0.712 |
| - Self-MM Yu et al. [2021] | >110M | 0.713 |
| - MMM Han et al. [2021a] | >110M | 0.700 |
| T5-based model | | |
| - UniMSE Hu et al. [2022] | >231M | 0.691 |
| RoBERTa-based model | | |
| - VAE-AMDT Wang et al. [2022] | >355M | 0.716 |
| VideoAdviser (ours) | | |
| - Student (BERT) | 110M | 0.704 |
| - Student (RoBERTa-Base) | 125M | 0.660 |
| - Student (RoBERTa-Large) | 361M | 0.568 |

5.6.4 Effectiveness of dataset size

In general, the larger the dataset, the better the performance. We trained *VideoAdviser* with a combination of the MOSI and MOSEI datasets to see if we can further improve the performance. As the results indicated in Tab. 9, The model performs much better than those trained on individual datasets and suggests the efficacy of our approach for different dataset sizes.

5.6.5 Effectiveness of the step-distillation loss

We ablatively studied the effects of our proposed step-distillation loss for multimodal knowledge distillation in Tab. 10. Without the first step—distilling multimodal knowledge from a video-enhanced prompt logit to a video logit (see Fig. 2), the learned multimodal space of CLIP cannot be passed to the student model via the video logit, resulting poor student model performance. On the other hand, it improves the regular language model (w/o step-distillation) **4.2%** MAE score

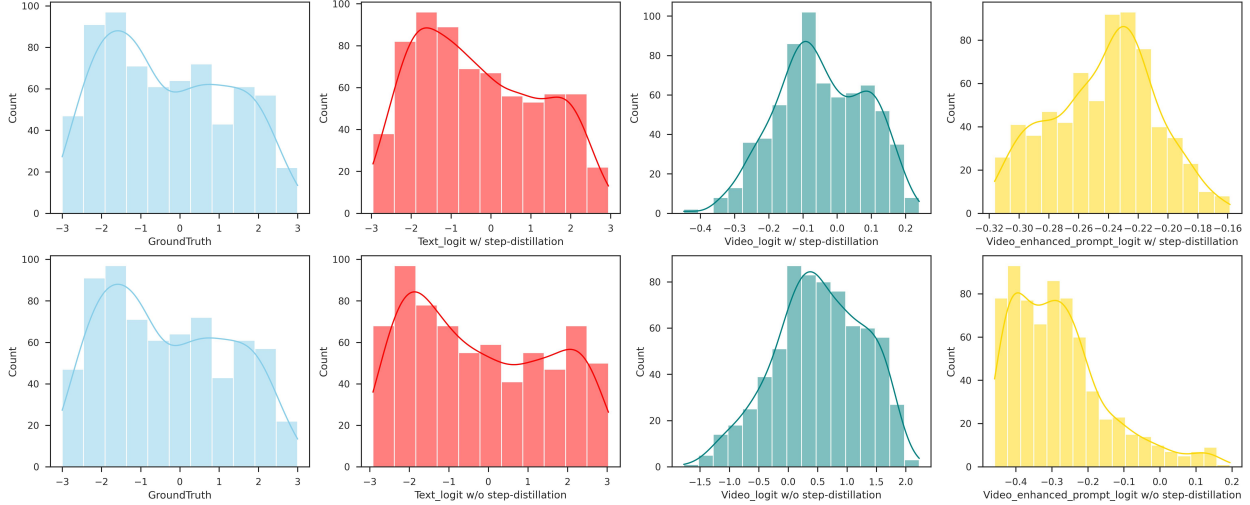


Figure 5: Visualization of logistic knowledge distribution with and without the step-distillation objective loss. The top row plots the histograms of logit by applying the step-distillation, and the bottom row indicates the vice-versa. The groundTruth indicates the label distribution, and text_logit indicates the predicted regression score of the student model. Our method using the step-distillation (the top) demonstrates a distribution of regression scores close to the groundTruth, affected by the knowledge distribution of the “video_logit” and “video_enhanced_prompt_logit”.

Table 6: Ablation results show the effects of components of the teacher model for multimodal knowledge distillation on MOSI dataset.

| Model | MOSI | | | |
|---------------------------------|--------------|-------------|-------------|-------------|
| | MAE | A^7 | A^2 | F1 |
| VideoAdviser (ours) | 0.568 | 51.3 | 87.7 | 87.9 |
| - w/o Facial expression encoder | 0.579 | 50.2 | 86.8 | 86.4 |
| - w/o Video-specific prompting | 0.570 | 50.1 | 88.1 | 87.7 |

Table 7: Effects in different student models. Our method improves the MAE score of pretrained language models by over **6.0** point on average.

| Model | MOSI | | |
|--------------------------------|--------------|-------------|-------------|
| | MAE | A^2 | F1 |
| Teacher (CLIP-based model) | - | 57.3 | - |
| BERT w/o teacher | 0.753 | 84.1 | 83.6 |
| Student (BERT) | 0.704 | 84.7 | 83.8 |
| RoBERTa-Base w/o teacher | 0.719 | 84.6 | 84.3 |
| Student (RoBERTa-Base) | 0.660 | 85.4 | 84.6 |
| RoBERTa-Large w/o teacher | 0.660 | 87.3 | 87.3 |
| Student (RoBERTa-Large) | 0.568 | 87.7 | 87.9 |

and suggests the effectiveness of the second step—distilling the knowledge of the video logit from the teacher model to the student model. Moreover, by optimizing the first and second steps, our proposed method outperforms a cutting-edge contrastive representation distillation method (CRD) Tian et al. [2020] that proposed a contrastive-based objective for transferring knowledge between deep networks. Compared to the CRD which is designed to model mutual information across dimensions of the knowledge representations, Our proposed step-distillation applies MSE to mapping mutual information across modalities via one-dimensional logits (*i.e.*, video-enhanced prompt logit, video logit, and text logit). Our method performs better than CRD in transferring regression information for multimodal knowledge distillation.

Table 8: Ablation results show the effects of step-distillation on audio and video modalities for VEGAS. Here, “w/ video distillation” indicates that the step-distillation is only adopted for the visual modality of the student model, “w/ audio distillation” indicates the other side, and “w/ audio and video distillation” indicates both sides (see Fig. 4).

| Model | VEGAS | | |
|------------------------------------|--------------|--------------|--------------|
| | A→V | V→A | Average |
| baseline (EICS Zeng et al. [2023]) | 0.797 | 0.779 | 0.788 |
| VideoAdviser (ours) | | | |
| -w/ video distillation | 0.794 | 0.810 | 0.802 |
| -w/ audio distillation | 0.791 | 0.815 | 0.803 |
| -w/ (audio and video) distillation | 0.825 | 0.819 | 0.822 |

Table 9: Results of *VideoAdviser* trained with a combination of MOSI and MOSEI datasets. The model performs much better for both the MOSI and MOSEI test sets. Here, (*) denotes the result of the model trained on the individual dataset.

| Test dataset | MAE | A^7 | A^2 |
|--------------|----------------------|--------------------|----------------------|
| MOSI | 0.546 (0.568) | 51.3 (51.3) | 88.5 (87.7) |
| MOSEI | 0.491 (0.502) | 55.6 (54.5) | 84.2 (84.5) |
| MOSI+MOSEI | 0.502 | 54.79 | 85.05 |

In addition, we show comparison results of the proposed step-distillation loss with three widely-known distillation function KD Hinton et al. [2015], FitNet Romero et al. [2014] and PKT Passalis and Tefas [2018] in Tab. 11. KD and PKT are proposed to minimize the KL divergence between the probabilistic outputs of a teacher and student model. On the other hand, FitNet and our step-distillation aim at minimizing the L_2 distance for knowledge distillation. Compared to KD, FitNet and PKT are one-step distillation loss functions, whereas our step-distillation performs two-step distillation, with the aim of transferring multimodal knowledge across multiple scales. To achieve a fair comparison, we adapted these three approaches to our problem setting of two-step distillation. As the results indicated in Tab. 11, the step-distillation outperforms other approaches and suggests its efficacy on multimodal knowledge distillation. We noted that the PKT-based two-step distillation achieves a compatible score with ours. We consider that audio-visual tasks focus on distilling multimodal knowledge of categorical audio events rather than fine-grained regressional knowledge so that transferring probabilistic knowledge of each category can also work well. Compared to KD which utilized the softmax function to obtain probabilistic knowledge, PKT adopted the cos-similarity function to better obtain dimension-level correlation with the probabilistic knowledge.

We further illustrate the logistic knowledge distribution with and without the step-distillation loss in Fig. 5. Compared to the “Text_logit w/o step-distillation” that plots the histogram of regression scores without performing the step-distillation, “Text_logit w/ step-distillation” is close to the groundTruth label distribution. Especially the distribution in the range of $[-1, 1]$ is strongly affected by the teacher model. Because the “Video_logit w/o step-distillation” distributes in the range of $[-1.5, 2]$ and the “Video_enhanced_prompt_logit w/o step-distillation” distributes in the range of $[-0.4, 0.2]$, by performing the step-distillation, the predicted regression score produced by the student model can be affected by the gap of these different distributions, and demonstrate that our proposed step-distillation is effective for multimodal knowledge distillation.

5.7 Significance Testing

We tested the stability of the performance improvement by *VideoAdviser* using the Almost Stochastic Order test (ASO) Del Barrio et al. [2018], Dror et al. [2019] as implemented by Ulmer et al. [2022]. We compared three models, *VideoAdviser* (ours), *VideoAdviser* w/o step-distillation (baseline), and CRD based on five random seeds each using ASO with a confidence level of $\alpha = 0.05$. ASO computes a score (ϵ_{\min}) indicated in Tab. 12 to represent how far the first model is from being significantly better with respect to the second. $\epsilon_{\min} = 0$ represents truly stochastic dominance and $\epsilon_{\min} < 0.5$ represents almost stochastic dominance.

Table 10: Ablation results show the effects of the proposed step-distillation loss for MOSI.

| Model | MOSI | | | |
|-------------------------------|--------------|-------------|-------|-------------|
| | MAE | A^7 | A^2 | F1 |
| CRD Tian et al. [2020] | 0.617 | 48.8 | 86.3 | 85.9 |
| VideoAdviser (ours) | | | | |
| - w/o step-distillation | 0.660 | 45.5 | 87.3 | 87.3 |
| - w/o step-distillation:step1 | 0.618 | 49.0 | 86.5 | 86.3 |
| - w/ step-distillation | 0.568 | 51.3 | 87.7 | 87.9 |

Table 11: Comparison results between widely-known knowledge distillation loss and the proposed step-distillation loss for VEGAS.

| Model | VEGAS | | |
|-------------------------------|--------------|--------------|--------------|
| | A→V | V→A | Average |
| KD Hinton et al. [2015] | 0.783 | 0.612 | 0.701 |
| FitNet Romero et al. [2014] | 0.803 | 0.781 | 0.792 |
| PKT Passalis and Tefas [2018] | 0.824 | 0.807 | 0.816 |
| step-distillation (ours) | 0.825 | 0.819 | 0.822 |

Table 12: ASO scores of models with different distillation objectives studied in Sec. 5.6. For “VideoAdviser (ours) → baseline”, $\epsilon_{\min} = 0$ indicates that VideoAdviser (ours) consistently outperform baseline. Here, the baseline denotes VideoAdviser (ours) w/o step-distillation.

| Model | ASO score (ϵ_{\min}) |
|--------------------------------|---------------------------------|
| VideoAdviser (ours) → baseline | 0 |
| VideoAdviser (ours) → CRD | 0 |
| CRD → baseline | 0.02 |

6 Conclusion

We proposed a novel multimodal knowledge distillation method, *VideoAdviser*, which leverages the strengths of learned multimodal space of the CLIP-based teacher model and large-scale parameters of the RoBERTa-based student model to perform multimodal knowledge transfer by optimizing a step-distillation objective loss. In the evaluation of two multimodal tasks, our method significantly outperforms SoTA methods up to **12.3%** MAE score with a single modal encoder used in inference for video-level sentiment analysis, and **3.4%** mAP for audio-visual retrieval tasks, suggesting its strengths in high efficiency-performance. Ablation studies further demonstrate the efficacy of our proposed step-distillation objective loss in improving multimodal knowledge distillation. In the next step, we will adapt meta-learning to further explore the capability of multimodal transfer learning in a few-shot setting.

References

- Fuzhen Zhuang, Zhiyuan Qi, Keyu Duan, Dongbo Xi, Yongchun Zhu, Hengshu Zhu, Hui Xiong, and Qing He. A comprehensive survey on transfer learning. *Proc. IEEE*, 109(1):43–76, 2021. doi:10.1109/JPROC.2020.3004555.
- Devamanyu Hazarika, Roger Zimmermann, and Soujanya Poria. Misa: Modality-invariant and-specific representations for multimodal sentiment analysis. *arXiv preprint arXiv:2005.03545*, 2020.
- Yinhan Liu, Myle Ott, Naman Goyal, Jingfei Du, Mandar Joshi, Danqi Chen, Omer Levy, Mike Lewis, Luke Zettlemoyer, and Veselin Stoyanov. Roberta: A robustly optimized bert pretraining approach. *ArXiv*, 2019.
- Tom Brown, Benjamin Mann, Nick Ryder, Melanie Subbiah, Jared D Kaplan, Prafulla Dhariwal, Arvind Neelakantan, Pranav Shyam, Girish Sastry, Amanda Askell, Sandhini Agarwal, Ariel Herbert-Voss, Gretchen Krueger, Tom Henighan, Rewon Child, Aditya Ramesh, Daniel Ziegler, Jeffrey Wu, Clemens Winter, Chris Hesse, Mark Chen, Eric Sigler, Mateusz Litwin, Scott Gray, Benjamin Chess, Jack Clark, Christopher Berner, Sam McCandlish, Alec

- Radford, Ilya Sutskever, and Dario Amodei. Language models are few-shot learners. In *NeurIPS*, volume 33, pages 1877–1901, 2020.
- Alexey Dosovitskiy, Lucas Beyer, Alexander Kolesnikov, Dirk Weissenborn, Xiaohua Zhai, Thomas Unterthiner, Mostafa Dehghani, Matthias Minderer, Georg Heigold, Sylvain Gelly, Jakob Uszkoreit, and Neil Houlsby. An image is worth 16x16 words: Transformers for image recognition at scale. *ICLR*, 2021.
- Alec Radford, Jong Wook Kim, Chris Hallacy, Aditya Ramesh, Gabriel Goh, Sandhini Agarwal, Girish Sastry, Amanda Askell, Pamela Mishkin, Jack Clark, Gretchen Krueger, and Ilya Sutskever. Learning transferable visual models from natural language supervision. In *ICML*, 2021.
- Liqiang Nie, Leigang Qu, Dai Meng, Min Zhang, Qi Tian, and Alberto Del Bimbo. Search-oriented micro-video captioning. In *MM*, page 3234–3243, 2022. ISBN 9781450392037. doi:10.1145/3503161.3548180.
- Liangli Zhen, Peng Hu, Xi Peng, Rick Siow Mong Goh, and Joey Tianyi Zhou. Deep multimodal transfer learning for cross-modal retrieval. *IEEE Trans. Neural Netw. Learn. Syst.*, 33(2):798–810, 2022. doi:10.1109/TNNLS.2020.3029181.
- Samuel Albanie, Arsha Nagrani, Andrea Vedaldi, and Andrew Zisserman. Emotion recognition in speech using cross-modal transfer in the wild. In *MM*, page 292–301, 2018. ISBN 9781450356657. doi:10.1145/3240508.3240578.
- Wenmeng Yu, Hua Xu, Yuan Ziqi, and Wu Jiele. Learning modality-specific representations with self-supervised multi-task learning for multimodal sentiment analysis. In *AAAI*, 2021.
- Wei Han, Hui Chen, and Soujanya Poria. Improving multimodal fusion with hierarchical mutual information maximization for multimodal sentiment analysis. In *EMNLP*, pages 9180–9192, 2021a. doi:10.18653/v1/2021.emnlp-main.723.
- Guimin Hu, Ting-En Lin, Yi Zhao, Guangming Lu, Yuchuan Wu, and Yongbin Li. UniMSE: Towards unified multimodal sentiment analysis and emotion recognition. In *EMNLP*, pages 7837–7851, 2022.
- Donghuo Zeng, Yi Yu, and Keizo Oyama. Deep triplet neural networks with cluster-cca for audio-visual cross-modal retrieval. *ACM Trans. Multimedia Comput. Commun. Appl.*, 16(3), 2020. ISSN 1551-6857. doi:10.1145/3387164.
- Liangli Zhen, Peng Hu, Xu Wang, and Dezhong Peng. Deep supervised cross-modal retrieval. In *CVPR*, pages 10386–10395, 2019. doi:10.1109/CVPR.2019.01064.
- Ning Han, Jingjing Chen, Guangyi Xiao, Yawen Zeng, Chuhao Shi, and Hao Chen. Visual spatio-temporal relation-enhanced network for cross-modal text-video retrieval. *arXiv preprint arXiv:2110.15609*, 2021b.
- Donghuo Zeng, Yanan Wang, Jianming Wu, and Kazushi Ikeda. Complete cross-triplet loss in label space for audio-visual cross-modal retrieval. In *ISM*, pages 1–9, 2022. doi:10.1109/ISM55400.2022.00007.
- Li He, Xing Xu, Huimin Lu, Yang Yang, Fumin Shen, and Heng Tao Shen. Unsupervised cross-modal retrieval through adversarial learning. In *ICME*, pages 1153–1158, 2017. doi:10.1109/ICME.2017.8019549.
- Bokun Wang, Yang Yang, Xing Xu, Alan Hanjalic, and Heng Tao Shen. Adversarial cross-modal retrieval. In *MM*, page 154–162, 2017. ISBN 9781450349062. doi:10.1145/3123266.3123326.
- Jian Zhang, Yuxin Peng, and Mingkuan Yuan. Unsupervised generative adversarial cross-modal hashing. In *AAAI*, 2017.
- Yanan Wang, Jianming Wu, Kazuaki Furumai, Shinya Wada, and Satoshi Kurihara. Vae-based adversarial multimodal domain transfer for video-level sentiment analysis. *IEEE Access*, 10:51315–51324, 2022. doi:10.1109/ACCESS.2022.3174215.
- Geoffrey Hinton, Oriol Vinyals, and Jeff Dean. Distilling the knowledge in a neural network. *arXiv preprint arXiv:1503.02531*, 2015.
- Saurabh Gupta, Judy Hoffman, and Jitendra Malik. Cross modal distillation for supervision transfer. In *CVPR*, pages 2827–2836, 2016. doi:10.1109/CVPR.2016.309.
- Fida Mohammad Thoker and Juergen Gall. Cross-modal knowledge distillation for action recognition. In *ICIP*, pages 6–10, 2019. doi:10.1109/ICIP.2019.8802909.
- Xiaoqi Jiao, Yichun Yin, Lifeng Shang, Xin Jiang, Xiao Chen, Linlin Li, Fang Wang, and Qun Liu. TinyBERT: Distilling BERT for natural language understanding. In *EMNLP*, pages 4163–4174, 2020. doi:10.18653/v1/2020.findings-emnlp.372.
- Lu Hou, Zhiqi Huang, Lifeng Shang, Xin Jiang, Xiao Chen, and Qun Liu. Dynabert: Dynamic bert with adaptive width and depth. In *NeurIPS*, 2020. ISBN 9781713829546.
- Boxiao Pan, Haoye Cai, De-An Huang, Kuan-Hui Lee, Adrien Gaidon, Ehsan Adeli, and Juan Carlos Niebles. Spatio-temporal graph for video captioning with knowledge distillation. In *CVPR*, pages 10870–10879, 2020.

- Zhishan Li, Ying Nie, Kai Han, Jianyuan Guo, Lei Xie, and Yunhe Wang. A transformer-based object detector with coarse-fine crossing representations. In *NeurIPS*, 2022.
- Licheng Jiao, Jie Gao, Xu Liu, Fang Liu, Shuyuan Yang, and Biao Hou. Multiscale representation learning for image classification: A survey. *IEEE Trans. Arti. Intell.*, 4(1):23–43, 2023. doi:10.1109/TAI.2021.3135248.
- Bolin Ni, Houwen Peng, Minghao Chen, Songyang Zhang, Gaofeng Meng, Jianlong Fu, Shiming Xiang, and Haibin Ling. Expanding language-image pretrained models for general video recognition. 2022.
- Xiuye Gu, Tsung-Yi Lin, Weicheng Kuo, and Yin Cui. Open-vocabulary detection via vision and language knowledge distillation. *arXiv preprint arXiv:2104.13921*, 2021.
- Yonglong Tian, Dilip Krishnan, and Phillip Isola. Contrastive representation distillation. In *ICLR*, 2020.
- Lin Wang and Kuk-Jin Yoon. Knowledge distillation and student-teacher learning for visual intelligence: A review and new outlooks. *IEEE Trans. Pattern Anal. Mach. Intell.*, 44(6):3048–3068, 2022. doi:10.1109/TPAMI.2021.3055564.
- Yanan Wang, Jianming Wu, Panikos Heracleous, Shinya Wada, Rui Kimura, and Satoshi Kurihara. Implicit knowledge injectable cross attention audiovisual model for group emotion recognition. In *ICMI*, page 827–834, 2020a. ISBN 9781450375818. doi:10.1145/3382507.3417960.
- Yanan Wang, Jianming Wu, Jinfa Huang, Gen Hattori, Yasuhiro Takishima, Shinya Wada, Rui Kimura, Jie Chen, and Satoshi Kurihara. Ldnn: Linguistic knowledge injectable deep neural network for group cohesiveness understanding. In *ICMI*, page 343–350, 2020b. ISBN 9781450375818. doi:10.1145/3382507.3418830.
- Ioana Croitoru, Simion-Vlad Bogolin, Marius Leordeanu, Hailin Jin, Andrew Zisserman, Samuel Albanie, and Yang Liu. Teachtex: Crossmodal generalized distillation for text-video retrieval. In *ICCV*, pages 11563–11573, 2021. doi:10.1109/ICCV48922.2021.01138.
- Wenliang Dai, Lu Hou, Lifeng Shang, Xin Jiang, Qun Liu, and Pascale Fung. Enabling multimodal generation on CLIP via vision-language knowledge distillation. In *ACL*, pages 2383–2395, 2022. doi:10.18653/v1/2022.findings-acl.187.
- Amir Zadeh, Rowan Zellers, Eli Pincus, and Louis-Philippe Morency. Mosi: Multimodal corpus of sentiment intensity and subjectivity analysis in online opinion videos. *ArXiv*, 2016.
- AmirAli Bagher Zadeh, Paul Pu Liang, Soujanya Poria, Erik Cambria, and Louis-Philippe Morency. Multimodal language analysis in the wild: CMU-MOSEI dataset and interpretable dynamic fusion graph. In *ACL*, pages 2236–2246, 2018. doi:10.18653/v1/P18-1208.
- Nikhil Rasiwasia, Dhruv Mahajan, Vijay Mahadevan, and Gaurav Aggarwal. Cluster Canonical Correlation Analysis. In *AISTATS*, volume 33, pages 823–831, 2014.
- Donghuo Zeng, Yi Yu, and Keizo Oyama. Audio-visual embedding for cross-modal music video retrieval through supervised deep cca. In *ISM*, pages 143–150, 2018. doi:10.1109/ISM.2018.00-21.
- Zhedong Zheng, Liang Zheng, Michael Garrett, Yi Yang, Mingliang Xu, and Yi-Dong Shen. Dual-path convolutional image-text embeddings with instance loss. *ACM Trans. Multimedia Comput. Commun. Appl.*, 16(2), 2020. ISSN 1551-6857. doi:10.1145/3383184.
- Donghuo Zeng, Jianming Wu, Gen Hattori, Rong Xu, and Yi Yu. Learning explicit and implicit dual common subspaces for audio-visual cross-modal retrieval. *ACM Trans. Multimedia Comput. Commun. Appl.*, 19(2s), 2023. ISSN 1551-6857. doi:10.1145/3564608.
- Tadas Baltrušaitis, Peter Robinson, and Louis-Philippe Morency. Openface: An open source facial behavior analysis toolkit. In *WACV*, 2016.
- S. Albanie and A. Vedaldi. Learning grimaces by watching tv. In *BMVC*, 2016.
- Omkar M. Parkhi, Andrea Vedaldi, and Andrew Zisserman. Deep face recognition. In *BMVC*, 2015.
- Ashish Vaswani, Noam Shazeer, Niki Parmar, Jakob Uszkoreit, Llion Jones, Aidan N Gomez, Łukasz Kaiser, and Illia Polosukhin. Attention is all you need. In *NeurIPS*, 2017.
- Yipin Zhou, Zhaowen Wang, Chen Fang, Trung Bui, and Tamara L Berg. Visual to sound: Generating natural sound for videos in the wild. In *CVPR*, pages 3550–3558, 2018. doi:10.1109/CVPR.2018.00374.
- Wasifur Rahman, Md Kamrul Hasan, Sangwu Lee, AmirAli Bagher Zadeh, Chengfeng Mao, Louis-Philippe Morency, and Ehsan Hoque. Integrating multimodal information in large pretrained transformers. In *ACL*, pages 2359–2369, 2020. doi:10.18653/v1/2020.acl-main.214.
- Diederik P. Kingma and Jimmy Ba. Adam: A method for stochastic optimization. *CoRR*, 2015.
- Colin Raffel, Noam Shazeer, Adam Roberts, Katherine Lee, Sharan Narang, Michael Matena, Yanqi Zhou, Wei Li, and Peter J. Liu. Exploring the limits of transfer learning with a unified text-to-text transformer. *J. Mach. Learn. Res.*, 21(1), 2020. ISSN 1532-4435.

- Soujanya Poria, Devamanyu Hazarika, Navonil Majumder, Gautam Naik, Erik Cambria, and Rada Mihalcea. MELD: A multimodal multi-party dataset for emotion recognition in conversations. In *ACL*, pages 527–536, 2019. doi:10.18653/v1/P19-1050.
- Carlos Busso, Murtaza Bulut, Chi-Chun Lee, Ebrahim (Abe) Kazemzadeh, Emily Mower Provost, Samuel Kim, Jeannette N. Chang, Sungbok Lee, and Shrikanth S. Narayanan. Iemocap: interactive emotional dyadic motion capture database. *Language Resources and Evaluation*, 2008.
- Yi Yu, Suhua Tang, Kiyoharu Aizawa, and Akiko Aizawa. Category-based deep cca for fine-grained venue discovery from multimodal data. *IEEE Trans. Neural Netw. Learn. Syst.*, 30(4):1250–1258, 2019. doi:10.1109/TNNLS.2018.2856253.
- Jacob Devlin, Ming-Wei Chang, Kenton Lee, and Kristina Toutanova. BERT: Pre-training of deep bidirectional transformers for language understanding. In *NAACL*, pages 4171–4186, 2019. doi:10.18653/v1/N19-1423.
- Adriana Romero, Nicolas Ballas, Samira Ebrahimi Kahou, Antoine Chassang, Carlo Gatta, and Yoshua Bengio. Fitnets: Hints for thin deep nets. *arXiv preprint arXiv:1412.6550*, 2014.
- Nikolaos Passalis and Anastasios Tefas. Learning deep representations with probabilistic knowledge transfer. In *ECCV*, 2018.
- Eustasio Del Barrio, Juan A Cuesta-Albertos, and Carlos Matrán. An optimal transportation approach for assessing almost stochastic order. In *The Mathematics of the Uncertain*, pages 33–44. Springer, 2018.
- Rotem Dror, Segev Shlomov, and Roi Reichart. Deep dominance - how to properly compare deep neural models. In *ACL*, pages 2773–2785, 2019. doi:10.18653/v1/p19-1266.
- Dennis Ulmer, Christian Hardmeier, and Jes Frelsen. deep-significance-easy and meaningful statistical significance testing in the age of neural networks. *arXiv preprint arXiv:2204.06815*, 2022.